THE JOURNAL OF PHYSICAL CHEMISTRY A
A JOURNAL OF THE AMERICAN CHEMICAL SOCIETY

pubs.acs.org/JPCA

Article

Highly Efficient Autoxidation of Triethylamine

Eva R. Kjærgaard, Kristian H. Møller, Torsten Berndt, and Henrik G. Kjaergaard*

Cite This: J. Phys. Chem. A 2023, 127, 8623−8632

Read Online

ACCESS | Metrics & More | Article Recommendations | Supporting Information

ABSTRACT: Autoxidation has been acknowledged as a major oxidation pathway in a broad range of atmospherically important compounds including isoprene and monoterpenes. More recently, autoxidation has also been identified as central and even dominant in the atmospheric oxidation of the rather small nonhydrocarbons dimethyl sulfide (DMS) and trimethylamine (TMA). Here, we find even faster autoxidation in the aliphatic amine triethylamine (TEA). The atmospherically dominating autoxidation leads to highly oxygenated and functionalized compounds. Products with as many as three hydroperoxy (OOH) groups and an O:C ratio larger than 1 are formed. We present theoretical multiconformer transition-state theory (MC-TST) calculations of the unimolecular reactions in the autoxidation following the OH + TEA reaction and calculate peroxy radical H-shift rate coefficients >20 s^{-1} for the first two generations of H-shifts. The efficient autoxidation in TEA is verified by the observation of the proposed highly oxidized products and radicals in flow-tube experiments. We find that the initial OH hydrogen abstraction at the α-carbon is strongly favored, with the β-carbon abstraction yield being less than a few percent.

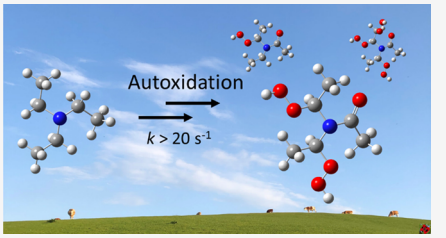

INTRODUCTION

Oxidation of the large amounts of volatile organic compounds (VOCs) emitted annually plays an essential role in the Earth's atmosphere. Much effort has been put into understanding the associated oxidation mechanisms, and within the past decade, autoxidation has been realized as an important process in this regard.[1,2] Initially, oxidation (by, for example, OH) of a VOC almost inevitably leads to the formation of a peroxy radical, RO_2. In autoxidation, a series of alternating unimolecular hydrogen shift (H-shift) or cyclization reactions followed by O_2 addition increase the oxygen content and the number of functional groups of the initial RO_2.[2,3] The autoxidation is often terminated by a loss of OH or HO_2, thereby contributing to HO_x recycling.[2,4] This uptake of O_2 and the addition of functional groups can lead to the formation of highly oxygenated organic molecules (HOMs), which have been linked to the formation and growth of aerosols.[4]

Autoxidation has been found to be important in a range of atmospherically relevant hydrocarbons, particularly isoprene and monoterpenes.[1,5,6] More recently, autoxidation was also identified in small sulfides and amines, somewhat surprising as autoxidation in propane and acetone is very slow.[7−13] The atmospheric oxidation of both sulfur and nitrogen compounds is important as both substance classes have been linked to particle formation.[14,15] Degradation of dimethylsulfonium propionate produced by marine algae in the oceans releases large amounts of dimethyl sulfide (DMS) into the atmosphere.[16] The autoxidation of dimethyl sulfide (DMS) and dimethyl disulfide (DMDS) leads to the formation of hydroperoxy thioformates.[10] In the case of DMS, the hydroperoxymethyl thioformate (HPMTF, $HOOCH_2SCHO$) has been identified both in the atmosphere[9] and in laboratory experiments.[8,13] In both cases, HPMTF was observed in a high yield. For DMDS, the analogous $HOOCH_2SSCHO$ has been observed in the laboratory.[10] The emission of aliphatic amines to the atmosphere arises mainly from livestock and biomass burning and is about 2 orders of magnitude lower than DMS emissions.[17] The aliphatic amine emission is dominated by trimethylamine (TMA).[18] The autoxidation in trimethylamine (TMA) leads to the formation of hydroperoxy amides, which have been observed in laboratory experiments.[11,12] Autoxidation has also been suggested for other aliphatic amines: dimethylamine (DMA), diethylamine (DEA), and triethylamine (TEA).[11,19]

In the atmosphere, the tertiary amine TMA will predominantly react with OH by hydrogen abstraction followed by O_2 addition to form an initial TMA peroxy radical. Until recently, it was assumed that this tertiary amine peroxy radical would react bimolecularly as illustrated in Figure 1 (in black), forming a range of possible nitrogen-containing compounds.[20] Peroxy and hydroperoxy amine formation would follow directly from the reaction of the tertiary amine peroxy radical with RO_2 and HO_2, respectively, whereas the bimolecular reaction with NO would form the TMA alkoxy radical. This alkoxy radical could form an amide (>N-(C═O)) or lose formaldehyde and subsequently react again bimolecularly to form nitrosamine (>N−NO), nitramine (>N−NO_2), or imine (−N═) com-

Received: June 28, 2023
Revised: September 19, 2023
Published: October 6, 2023

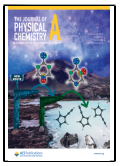

https://doi.org/10.1021/acs.jpca.3c04341
J. Phys. Chem. A 2023, 127, 8623−8632

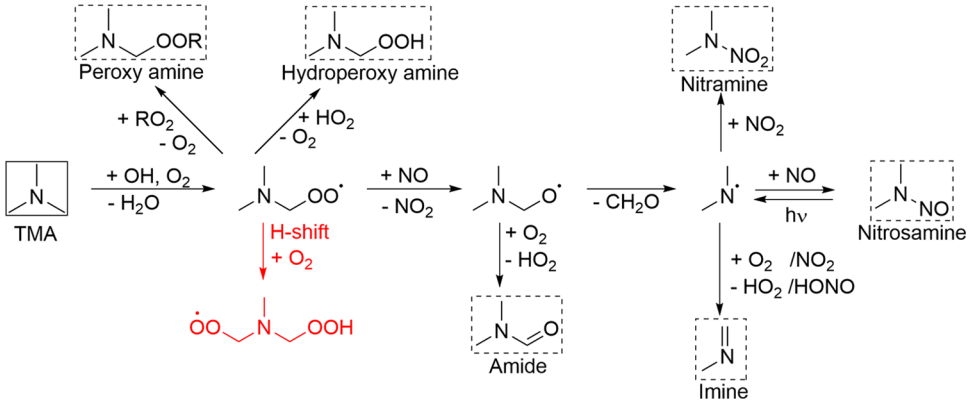

Figure 1. Reaction mechanism of trimethylamine (TMA, solid box) + OH. The fast H-shift reaction is shown in red. Previously proposed closed-shell products are shown in dashed boxes.

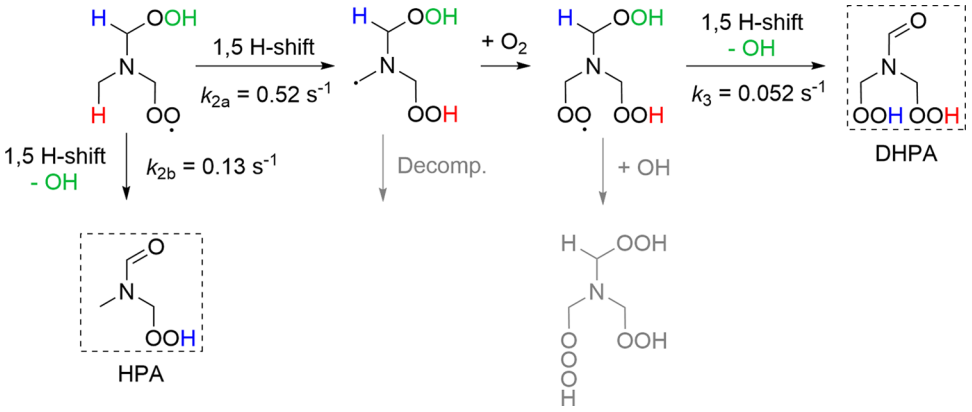

Figure 2. The TMA-derived hydroperoxy peroxy radical leads to the formation of a hydroperoxy amide (HPA) and a dihydroperoxy amide (DHPA) shown in dashed boxes. Both *E*/*Z* isomers of HPA exist but are not distinguished in the figure. The rate coefficients shown are calculated at 298.15 K with the approach described in the Method section.[11] The rate coefficients given here include both isomers. Selected atoms are colored to highlight the reaction pathways. Less important pathways are marked in gray.

pounds.[20] The nitrosamine and nitramine are suspected carcinogens and are of concern in connection with, e.g., amine leakage from carbon capture and storage facilities.[20]

However, it was recently found that the TMA peroxy radical has a fast unimolecular H-shift reaction (~3 s^{-1} at 298 K).[11,12] This fast H-shift will under most environmental conditions outrun the competing bimolecular reactions (NO, RO_2, OH, HO_2), which all react with rate coefficients of about 10^{-11} cm^3 $molecule^{-1}$ s^{-1}.[21] In pristine conditions, with an NO concentration of about 50 ppt, this leads to a pseudo-first-order reaction rate coefficient of the TMA peroxy radical of about 10^{-2} s^{-1}. In more polluted environments, the concentration of NO is larger, and the pseudo-first-order rate coefficient increases. However, even at an NO concentration of about 5 ppb, the pseudo-first-order bimolecular rate coefficient is unlikely to be higher than about 1 s^{-1}.[22] Thus, due to the fast H-shift, TMA will react with OH to form the hydroperoxy peroxy radical (Figure 1, red) in most environments. This hydroperoxy peroxy radical can either undergo bimolecular reactions or continue with subsequent H-shifts. The two possible subsequent 1,5 H-shifts are shown in Figure 2. Abstraction of the hydrogen on the carbon with the OOH group (Figure 2, blue hydrogen, k_{2b}) is the slower of the two and leads to the formation of a hydroperoxy amide (HPA). The abstraction from the methyl group (Figure 2, red hydrogen, k_{2a}) is calculated to be about a factor of 4 faster than k_{2b} and after another O_2 addition and 1,5 H-shift leads to the formation of a dihydroperoxy amide (DHPA).[11,12] The hydroperoxy amides, HPA and DHPA, as well as their precursor peroxy radicals have been detected in flow-tube experiments.[12] Formation of either of these amides results in OH recycling. It is somewhat surprising that $k_{2a} > k_{2b}$ since the additional OOH on the methyl group associated with k_{2b} has been found to accelerate H-shift reactions in hydrocarbon.[23] Very recently, peroxy radicals have been shown to react rather ubiquitously with OH to form hydrotrioxides, ROOOH; however, in the atmosphere, this will not be competitive with the 1,5 H-shift in this system.[24] In the TMA oxidation, the dihydroperoxy hydrotrioxide (Figure 2) was found to be rather stable and has been detected with chemical ionization mass spectroscopy in free-jet flow-tube experiments.[24]

Here, we investigate autoxidation in a larger tertiary amine, triethylamine (TEA), to investigate earlier suggestions that the H-shift reactions are faster in larger amines and that amides are generally formed in the atmospheric oxidation of tertiary amines.[11,19] We use theoretical multiconformer transition-state theory (MC-TST) to calculate the H-shift reaction rate coefficients for the peroxy radicals formed in the autoxidation of TEA. We compare the autoxidation following hydrogen abstraction from either the α- or β-position. Finally, the theoretical results are compared with those of flow-tube

https://doi.org/10.1021/acs.jpca.3c04341
J. Phys. Chem. A 2023, 127, 8623−8632

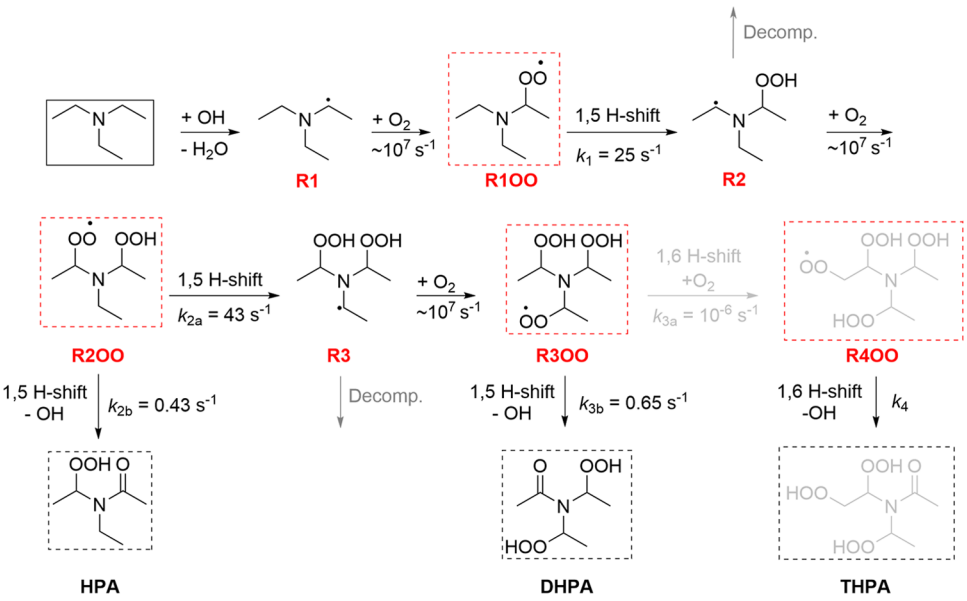

Figure 3. Dominant autoxidation mechanism of TEA (solid box) initiated by reaction with OH. The closed-shell products are shown in black dashed boxes, and the peroxy radicals are shown in red dashed boxes. Several minor routes have been left out. The rate coefficients shown are calculated at T = 298.15 K with the approach described in the Method section. Only the rate coefficient of the stereoisomer with the fastest H-shift is shown. Less important pathways are marked in gray.

experiments using chemical ionization mass spectrometry detection.

COMPUTATIONAL METHODS

Reaction rate coefficients of the unimolecular reactions in this study were calculated with a previously developed and tested multiconformer transition-state theory (MC-TST) approach.[25,26] This approach has yielded rate coefficients that are within a factor of 5 of the experimentally determined H-shift rate coefficients for a range of different measured peroxy radical H-shift reactions.[6,15,27]

The initial step of the approach is to optimize a conformer of the reactant and transition state (TS) for each reaction studied at the B3LYP/6-31+G(d) level in Gaussian 16 rev C.01.[28−31] A systematic conformational sampling is performed on the optimized structures using MMFF in Spartan'18, including the keyword "FFHINT=X∼∼+0" for radical structures to enforce a neutral charge on the radical atom, X.[32,33] Constraints are added to selected transition-state bond lengths during conformational sampling. For peroxy radical H-shift reactions, these are the O−O bond of the peroxy group, the O−H bond being formed, and the H−C bond being broken. For the decomposition reactions, we constrain the bond lengths of the two bonds being broken (O−O and N−C) as well as the two bonds going from single to double bonds (C−N and C−O).

The conformers found from the sampling are then optimized at the B3LYP/6-31+G(d) level in Gaussian 16. The optimized structures are compared to remove duplicates based on electronic energy differences below 1×10^{-5} Hartree and dipole moment differences below 1.5×10^{-2} Debye.[34] Additionally, an electronic energy cutoff of 2 kcal/mol is used to discard high-energy conformers. The remaining conformers are then further optimized at the ωB97X-D/aug-cc-pVTZ level.[35,36] The zero-point vibrational energy (ZPVE) correction is calculated from an ωB97X-D/aug-cc-pVTZ harmonic frequency calculation. For the lowest-energy conformers (ωB97X-D/aug-cc-pVTZ electronic energy + ZPVE) of the reactant and TS an ROHF-ROCCSD(T)-F12a/cc-pVDZ-F12 (abbreviated F12) single-point energy calculation was performed using MOLPRO2012.1 to obtain a more accurate barrier height.[37,38]

Tunneling is considered by performing a forward and reverse intrinsic reaction coordinate (IRC) calculation at the B3LYP/6-31+G(d) level with the keyword "calcall". The IRC starting points are the B3LYP/6-31+G(d) geometry of the TS conformer that is lowest in ZPVE-corrected ωB97X-D/aug-cc-pVTZ energy. The IRC endpoints are initially optimized at the B3LYP/6-31+G(d) level and subsequently at the ωB97X-D/aug-cc-pVTZ level. For H-shifts abstracting hydrogens from carbon atoms with a hydroperoxy group, the hydroperoxy group is constrained in the product to prevent OH loss. Finally, F12 single-point calculations are performed on the TS and IRC endpoints. We use the 1D Eckart tunneling approximation that takes as input; the forward and reverse IRC barrier heights calculated using the F12 electronic energies with the ωB97X-D/aug-cc-pVTZ ZPVE correction and the imaginary frequency of the lowest-energy TS conformer calculated at the ωB97X-D/aug-cc-pVTZ level.[39]

Rate coefficients (k) are calculated using the MC-TST equation[25,26]

$$k = \kappa \frac{k_B T}{h} \frac{\sum_i^{\text{TSconf.}} \exp\left(-\frac{\Delta E_i}{k_B T}\right) Q_{\text{TS}_i}}{\sum_j^{\text{Rconf.}} \exp\left(-\frac{\Delta E_j}{k_B T}\right) Q_{\text{R}_j}} \exp\left(-\frac{E_{\text{TS}} - E_{\text{R}}}{k_B T}\right)$$

where κ is the tunneling correction factor, k_B is the Boltzmann constant, T is the temperature, h is Planck's constant, Q_{TS_i} is the partition function (ωB97X-D) of the ith TS conformer, and ΔE_i is the energy (ωB97X-D) difference between the ith TS conformer and the lowest-energy TS conformer. E_{TS} is the energy (F12 with ωB97X-D ZPVE) of the lowest-energy TS conformer. The symbols are similarly defined for the reactant (R), with index j instead of i. All energies in the equation above

https://doi.org/10.1021/acs.jpca.3c04341
J. Phys. Chem. A 2023, 127, 8623−8632

are electronic energies including ZPVE correction. Reaction rate coefficients are calculated at 298.15 K under the harmonic oscillator and rigid rotor approximations and are high-pressure limit values. We calculate the rate coefficients for all unique (non enantiomer) stereoisomers where applicable.[40]

EXPERIMENTAL METHODS

Experiments were performed in a free-jet flow system at 295 ± 2 K, a relative humidity (RH) of <0.1%, and a pressure of 1 bar purified air for low-NO conditions, [NO] < 2×10^8 molecules cm^{-3}. The reaction time was 7.9 s, and the total flow was set at 100 L/min (STP). This setup allows investigations for almost wall-free conditions. More details on the experimental setup can be found elsewhere.[12] Briefly, the flow system consists of an outer tube (inner diameter: 16 cm) and an inner tube (outer diameter: 9.5 mm) with a nozzle of 3 mm inner diameter. Ozone or isopropyl nitrite (IPN) mixed with air (5 L min^{-1}, STP) is injected through the inner tube into the main gas stream (95 L min^{-1}, STP), which contains other reactants, i.e., tetramethylethylene (TME) and triethylamine (TEA), diluted in air. A series of TEA oxidation experiments were conducted with OH radicals produced from either ozonolysis of TME[41] or photolysis of IPN.[42] The concentrations of either TME and O_3 or IPN were varied to produce different OH concentrations. Chemical ionization-atmospheric pressure interface−time-of-flight (CI-API-TOF) mass spectrometry was applied for product analysis. Product ionization by pyruvate (CH_3COCOO^-) or iodide (I^-) was used for detection, both of which have been shown to be efficient ionization schemes in previous amine oxidation experiments.[12] Stated product concentrations and corresponding product yields represent lower limit values with an uncertainty of a factor of 2, which were obtained using a calculated calibration factor of 1.85×10^9 molecules cm^{-3}.[43,44]

RESULTS AND DISCUSSION

Reaction Mechanism for TEA + OH. The reaction of TEA with OH proceeds via hydrogen abstraction at either the α- or β-carbon position relative to the nitrogen atom (Figure S1). Abstraction at the α-carbon is expected to be favored due to the formation of a secondary alkyl radical and the fact that nitrogen seems to activate the nearby hydrogens. This is supported by results from previous experiments on ethylamine,[45] barrier height calculations,[19] and a hydrogen abstraction SAR.[46]

In Figure 3, we illustrate the dominant autoxidation mechanism of TEA, leading to the formation of highly oxidized (poly)-hydroperoxy peroxy radicals and (poly)-hydroperoxy amides. The hydrogen abstraction at the α-carbon is followed by fast O_2 addition (pseudo-first-order rate coefficient of about 10^7 s^{-1})[47] resulting in the formation of the initial peroxy radical (R1OO), which has three possible unimolecular reaction pathways (Figure S1): the 1,4 H-shift from the adjacent methyl group, a 1,6 H-shift from the other two methyl groups, and a 1,5 H-shift from the methylene groups (α-carbon). The 1,4 and 1,6 H-shifts are very slow with calculated rate coefficients (Figure S1 and Table S2) many orders of magnitude smaller than that of the preferred 1,5 H-shift (Figure 3). Even though the reverse reaction (k_{-1}) is fast (Table S2) and comparable to the addition of the O_2 to R2, this will have a very limited effect. The MC-TST calculated rate coefficient of the 1,5 H-shift is 25 s^{-1}, almost an order of magnitude faster than the calculated rate coefficient of the corresponding first H-shift in the TMA + OH system (2.9 s^{-1}). This trend is in agreement with results for hydrocarbons, where a methyl group substituent was found to enhance H-shift reaction rate coefficients by about an order of magnitude.[23] The calculated first-generation H-shifts in the autoxidation of di- and trimethylamine (DMA and TMA) and di- and triethylamines (DEA and TEA) are compared in Tables 1 and S1. All these first-generation 1,5 H-shifts in amines are significantly faster than the pseudo-first-order rate coefficient for bimolecular reaction with NO in pristine conditions (about 10^{-2} s^{-1}), and for the tertiary amines (TMA and TEA), they would outcompete the NO bimolecular reaction even in moderately polluted environments. Thus, for tertiary amines, autoxidation is likely the dominant atmospheric oxidation mechanism. These first-generation H-shifts in amines are orders of magnitude faster than the analogous reactions in hydrocarbons.[11]

Table 1. MC-TST Calculated Rate Coefficients (s^{-1}) for Peroxy Radical 1,5 H-Shifts in the OH Oxidation of Triethylamine (TEA), Trimethylamine (TMA), Diethylamine (DEA), and Dimethylamine (DMA)[a]

molecule	k_1	k_{2a}	k_{2b}
TEA	25	43 (*R,R*)	0.43 (*R,R*)
		7.1 (*R,S*)	0.034 (*R,S*)
TMA[b]	2.9	0.52	0.13
DEA[c]	5.4		0.37 (*R,R*)
			0.48 (*R,S*)
DMA[c]	0.33		0.011

[a]Rate coefficients are calculated at T = 298.15 K with the approach described in the Method section. [b]The rate coefficients for TMA include the formation of both E/Z isomers and are taken from refs 11,48 (ref 48 now in press). [c]The rate coefficients for DEA and DMA are taken from ref 11. The references employ the same level of theory as used here. The rate coefficient k_{2a} leads to an alkyl radical and k_{2b} is the 1,5 H-shift leading to the formation of a hydroperoxy amide (HPA) and loss of OH (Figure 3 for TEA).

The newly formed α-carbon-centered alkyl radical (R2, Figure 3) will either add O_2 to form another peroxy radical (R2OO) or undergo unimolecular decomposition to form two closed-shell products, $CH_3CH_2N{=}CHCH_3$ and $CH_3C(O)H$, and an OH radical (Figure S1). In a recent theoretical study, this decomposition channel was suggested to be a significant component of the autoxidation for both TMA (~30%) and TEA (~50%).[19] These calculations used the MESMER (Master Equation Solver for Multi-Energy Well Reactions) code to include the excess energy from the O_2 addition and ab initio calculations at the UCBS-QB3//M05/aug-cc-pVTZ level. In an earlier experimental study, the OH recycling from this decomposition channel in the TMA + OH reaction was found to account for only about 2% at 298 K from extrapolation of low-pressure experiments. The previous experimental study concluded that for TMA, this decomposition pathway ($CH_3N{=}CH_2$ + HC(O)H + OH) is not significant at 298 K and atmospheric pressure.[45] The experimental result is in good agreement with our previous calculation, which found a decomposition yield of 3% for TMA also modeling the excess energy from the O_2 addition with MESMER but with the ab initio calculations at the ROCCSD(T)-F12a/VDZ-F12//ωB97X-D/aug-cc-pVTZ

https://doi.org/10.1021/acs.jpca.3c04341
J. Phys. Chem. A 2023, 127, 8623−8632

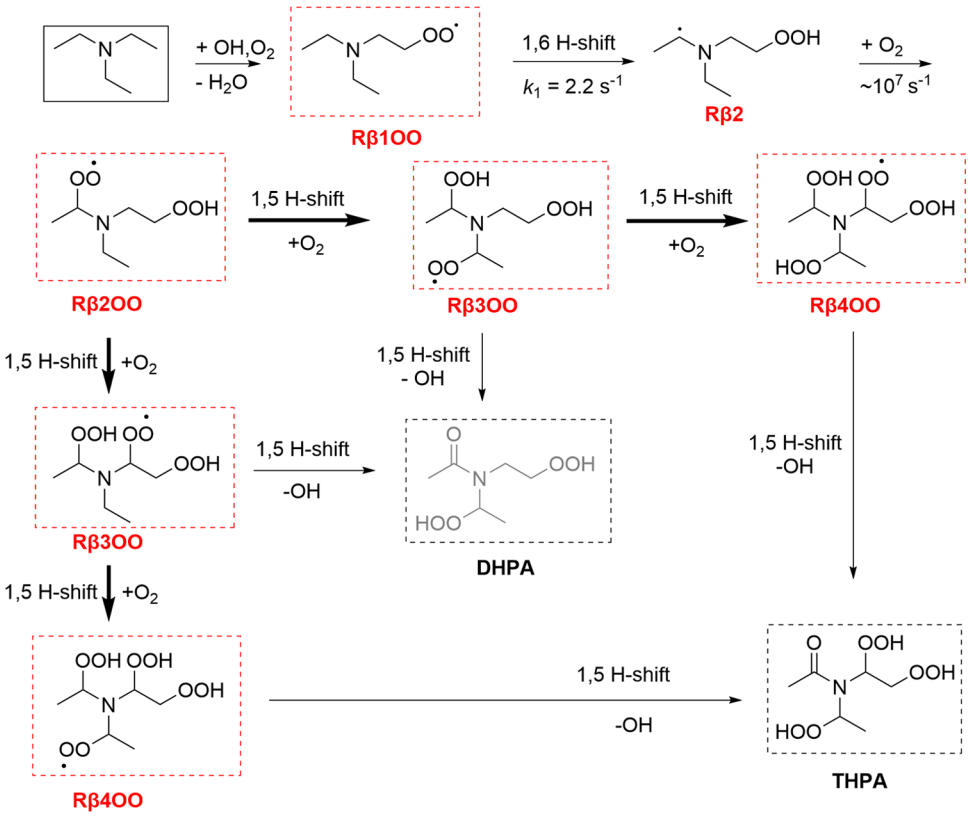

Figure 4. Suggested reaction mechanism for TEA (solid box) oxidation initiated by OH H-abstraction at the β-carbon. The rate coefficient is calculated at 298.15 K with the approach described. The bold arrows indicate fast 1,5 H-shifts with rate coefficients estimated to be about 10 s^{-1} and the thinner arrows 1,5 H-shifts with rate coefficients estimated to be about 0.1 s^{-1}. The closed-shell products are shown in black dashed boxes and the peroxy radicals are in red dashed boxes. Other comparable pathways leading to isomers of the same composition exist but are not shown. Less important pathways are marked in gray.

level.[11] The dissociation barrier is slightly smaller in the QB3 calculation compared to that in the F12 calculation, which is likely the reason for the higher yield from the QB3 results. Here, we have used the F12 level as in the previous work to estimate the dissociation yield.[11] Without excess energy, the decomposition reaction from R2 has an MC-TST (F12) calculated decomposition rate coefficient of 2.6×10^4 s^{-1}, which is insignificant compared to the pseudo-first-order reaction coefficients of $\sim 10^7$ s^{-1} for the O_2 addition reaction. The excess energy from the previous OH addition is mostly dissipated due to collisions.[49] We use MESMER[50] to simulate the excess energy from the O_2 addition. Assuming only the excess energy from the O_2 addition, we find a decomposition yield of about 1% (Figures S2 and S3) and hence we assume that R2 will mainly react with O_2 to form a new peroxy radical R2OO (Figure 3). We assume similar results from subsequent alkyl radicals and expect decomposition reactions to be insignificant compared with the results from the O_2 addition reactions.

Different stereoisomers can have significantly different H-shift rate coefficients.[5,27,40] The R2OO radical has two stereogenic centers, and we calculate the H-shift rate coefficients for both (*R*,*R*) and (*R*,*S*) stereoisomers (Table 1). Previously, in diethylamine (DEA), the two isomers were found to have comparable H-shift rate coefficients.[11] The R2OO radical can react *via* several unimolecular pathways. However, given the clear trend for the initial peroxy radical R1OO, we considered only the α-carbon sites. There are two possible second-generation 1,5 H-shifts, which include abstraction from an α-carbon (Figure 3 and Table S2). The 1,5 H-shift similar to that of R1OO is comparably very fast, calculated to be $k_{2a}(R,R) = 43$ s^{-1} and slightly slower for the other isomer with $k_{2a}(R,S) = 7$ s^{-1}. The other second-generation 1,5 H-shift is an abstraction of a hydrogen adjacent to a hydroperoxy group and leads to formation of a hydroperoxy amide (HPA, Figure 3) by subsequent decomposition recycling of OH. The formed HPA is analogous to the hydroperoxy amide formed in the TMA + OH system (Figure 2). Compared to the first-generation H-shift (k_1), this 1,5 H-shift is found to be significantly slower with rate coefficients of $k_{2b}(R,R) = 0.43$ s^{-1} and $k_{2b}(R,S) = 0.034$ s^{-1} (Table 1). The almost 2 orders of magnitude difference between k_{2a} and k_{2b}, is somewhat surprising. Similar results were found for the corresponding reactions in TMA, although with only a factor of 4 difference (Table 1).[11] In previous studies on hydrocarbons, a hydroperoxy group was found to increase the rate of H-shift reactions from the adjacent carbon by a factor of about 50.[23] The reason for the 2 orders of magnitude difference between k_{2a} and k_{2b} for TEA comes from the formation of hydrogen bonds in the reactant and transition states of the associated reaction (Figures S4−S6). The lowest-energy reactant is stabilized by an OOH-O hydrogen bond, which remains in the TS of the k_{2a} reaction but is not possible in the k_{2b} reaction. This hydrogen bond stabilizes the TS and thereby lowers the barrier height, as also seen in Table S2. In Table 1, we compare the calculated 1,5 H-shift rate coefficients for different secondary and tertiary amines. We find that both first- and second-generation 1,5 H-shift rate coefficients are faster in

https://doi.org/10.1021/acs.jpca.3c04341
J. Phys. Chem. A 2023, 127, 8623−8632

the ethyl-substituted amines for both the tertiary (TEA vs TMA) and secondary (DEA vs DMA) amines. In both tertiary amines, the abstraction of the hydrogen on the α-carbon without a hydroperoxy group is favored, $k_{2a} > k_{2b}$. Thus, for R2OO, the main reaction pathway will be the formation of the dihydroperoxy α-carbon-centered alkyl radical, R3 (Figure 3). Under pristine atmospheric conditions, the first- and second-generation 1,5 H-shifts in TEA are significantly faster than competing bimolecular reactions, and the TEA + OH reaction will lead to a significant yield of highly oxygenated amine-derived compounds. Even in moderately polluted environments, the formation of R3, which already has two hydroperoxy groups, will dominate the TEA + OH oxidation. For all of the hydroperoxy peroxy radicals, the hydroperoxy hydrogen(s) will be rapidly shifted between the different peroxy groups via H-shifts, but this will not impact the overall autoxidation mechanism.[51] The reverse reaction (k_{-2a}) is very fast (Table S2) and comparable to the O_2 addition to R3. Due to the significantly larger k_{2a} than k_{2b}, this fast reverse reaction is not sufficient to change the product formation significantly. This is in agreement with the experimental observation of large amounts of R3OO and DHPA formed compared to HPA within the 7.9 s of the flow-tube experiments.

Like R2, radical R3 can undergo either an O_2 addition to form another peroxy radical (R3OO) or unimolecular decomposition to form two closed-shell products $CH_3C(OOH)HN{=}CHCH_3$ and $CH_3C(O)H$ and an OH radical. Based on the results for TMA and our calculation for the decomposition of R2, we assume that the decomposition of R3 will also be a minor pathway and that R3OO will be formed predominantly. The peroxy radical R3OO can undergo a 1,5 H-shift abstracting a hydrogen on an α-carbon with an OOH group attached with subsequent loss of OH and formation of a dihydroperoxy amide (DHPA, Figure 3). For this reaction, a larger difference in rate coefficients is observed between the diastereomers than was the case for R2OO, with the fastest and slowest reactions differing by more than a factor of 300 (Table S2). The calculated rate coefficient for the fastest of these H-shifts is $k_{3b} = 0.65\ s^{-1}$ and is thus competitive with bimolecular reactions in the atmosphere. In contrast, the slowest diastereomer has a calculated rate coefficient of $k_{3b} = 2.1 \times 10^{-3}\ s^{-1}$ and is thus generally atmospherically uncompetitive. As such, this could represent a bifurcation between the mechanisms of different diastereomers. A 1,6 H-shift abstracting a hydrogen from a methyl group is also possible for R3OO and would after O_2 addition lead to the formation of R4OO, which could undergo a 1,6 H-shift with subsequent loss of OH leading to the formation of a trihydroperoxy amide (THPA, Figure 3). However, the calculated rate coefficient for the initial 1,6 H-shift is very slow, $k_{3a} = 10^{-6}\ s^{-1}$ (fastest isomer, Table S2). We have not calculated the rate coefficient of the final 1,6 H-shift from R4OO, k_4, due in part to the large number of initial conformers ($\sim 10^5$), the size of its F12 single-point calculation, and the fact that R4OO is unlikely to be formed.

Autoxidation of TEA following abstraction from the less favored β-carbon site is expected to lead to compounds comparable to those for the α-carbon site abstraction (Figure 4 and Section S2). We have calculated the rate coefficients for the possible first-generation H-shifts in the RO_2 radical (Rβ1OO) arising from hydrogen abstraction at the β-carbon (Figure S7 and Table S3). The 1,6 H-shift is the fastest H-shift with a rate coefficient of $2.2\ s^{-1}$ and is the only one that needs to be considered. The reverse reaction (k_{-1}) is fast (Table S3) but not competitive with the O_2 addition to Rβ2. While this 1,6 H-shift is fast, it is an order of magnitude slower than the first-generation 1,5 H-shift of the RO_2 arising from the dominant α-carbon abstraction (R1OO, k_1). We assume that decomposition is minor, and following the 1,6 H-shift, O_2 will add to the alkyl radical to form a hydroperoxy peroxy radical, Rβ2OO (Figure 4). The Rβ2OO radical has two possible 1,5 H-shifts that are both expected to be fast. We have not calculated these rate coefficients, but based on the results from nearly identical reactions in the α-abstraction pathway, they are expected to have rate coefficients on the order of $10\ s^{-1}$. The formed dihydroperoxy peroxy radicals (Rβ3OO) have the possibility of two 1,5 H-shifts akin to those of R2OO (Figure 3) and similar to R2OO, the expected slower of the two H-shift (on the order of $0.1\ s^{-1}$) will lead to a DHPA. This DHPA has a different structure to that originating from the α-abstraction pathway but will have the same mass and functional groups. The faster of the two 1,5 H-shifts, again with an estimated rate coefficient on the order of $10\ s^{-1}$, will lead to trihydroperoxy peroxy radicals (Rβ4OO). These can undergo a 1,5 H-shift to form THPA (Figure 4). We estimate the rate coefficient of this 1,5 H-shift to be on the order of $0.1\ s^{-1}$. This is a plausible route to the formation of a trihydroperoxy peroxy radical and the closed-shell THPA on a reasonable time scale. In the α-abstraction channel, the formation of THPA is hindered by a slow 1,6 H-shift. By contrast, for the β-abstraction, THPA follows from an initial fast 1,6 H-shift ($2.2\ s^{-1}$) followed by two likely faster 1,5 H-shifts (likely $\sim 10\ s^{-1}$) and a final medium fast 1,5 H-shift ($\sim 0.1\ s^{-1}$). Other THPA structures than the ones shown in Figures 3 and 4 are also possible, e.g., via fast hydroperoxy−peroxy H-shifts of the intermediate peroxy radicals, and will all have the same mass and functional groups.[51] Thus, THPA is expected to form from the minor β-abstraction channel, whereas DHPA is predominantly formed from the α-abstraction channel. The trihydroperoxy amide (THPA) has an astounding three hydroperoxy groups in the same molecule and an O:C ratio of 7:6.

It is clear that the atmospheric oxidation of tertiary amines will predominantly happen via very fast autoxidation, leading to highly functionalized (poly)-hydroperoxy amides. This is consistent with observations that only tertiary amines contribute significantly to the formation of secondary organic aerosols (SOAs) by mechanisms involving atmospheric oxidation and growth rather than the formation of salts.[52−54]

Product Detection in the TEA + OH Reaction. In the flow-tube experiments, we detected several radicals and closed-shell products of the TEA and OH reaction. In Figure 5, we show a product mass spectrum from the TEA + OH reaction, using pyruvate for product ionization and OH production from TME ozonolysis. A similar product distribution was observed in an experiment, applying OH generation via IPN photolysis and product detection by means of iodide ionization (Figure S8). The good agreement suggests a limited influence of the experimental parameters on the observed product formation. We detected masses consistent with the three hydroperoxy amides, HPA, DHPA, and THPA, which are highlighted in black dashed boxes in Figures 3 and 4. Based on the calculations, we suggest that the HPA and DHPA compounds arise predominantly from the α-abstraction channel, whereas THPA arises from the minor β-abstraction channel.

https://doi.org/10.1021/acs.jpca.3c04341
J. Phys. Chem. A 2023, 127, 8623−8632

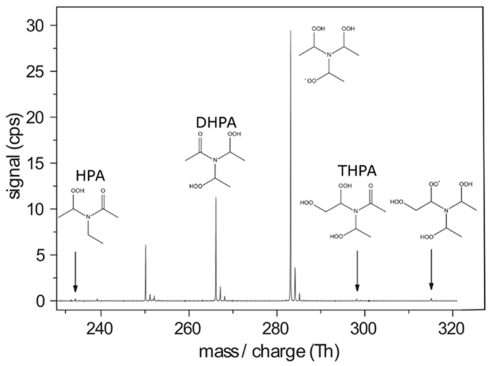

Figure 5. Product mass spectrum for the reaction of OH + TEA using pyruvate (CH_3COCOO^-) ionization for detection. The products appear as an adduct: (product)CH_3COCOO^-. OH radicals were produced from tetramethylethylene (TME) ozonolysis. Reactant concentrations were $[O_3] = 3.1 \times 10^{11}$, $[TME] = 5.18 \times 10^{11}$, and $[TEA] = 3.17 \times 10^{11}$ molecules cm^{-3} and a reaction time of 7.9 s at $T = 295$ K. The products shown are consistent with the observed masses and the proposed mechanism but signals likely include multiple isomers.

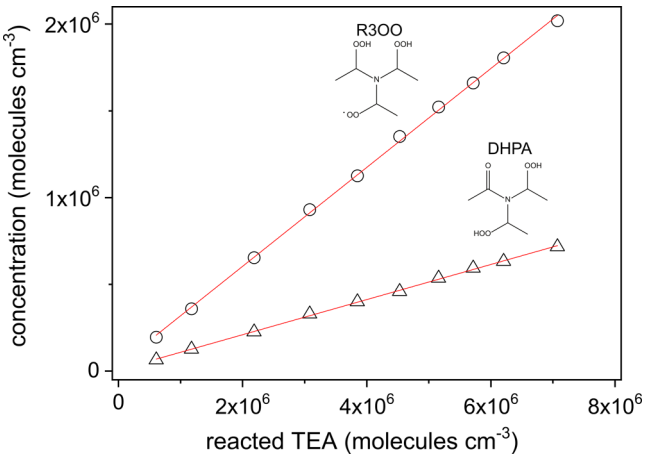

Figure 6. Dihydroperoxy peroxy radical (R3OO, circles, 323 Th) and dihydroperoxy amide (DHPA, triangles, 306 Th) formation from TEA + OH. Tetramethylethylene (TME) ozonolysis was used to generate OH radicals and iodide (I^-) was used as the reagent ion. The reactant concentrations were $[O_3] = 1.5 \times 10^{10}$, $[TME] = (5.18–104) \times 10^9$, and $[TEA] = 2.11 \times 10^{11}$ molecules cm^{-3} and a reaction time of 7.9 s and 295 K. The given concentrations represent lower limit values. The resulting lower limit formation yields are 0.29 for R3OO and 0.10 for DHPA.

In addition to the closed-shell amides, we detected masses consistent with the formation of peroxy radicals with two and three hydroperoxy groups (R3OO/Rβ3OO and R4OO/Rβ4OO). These are highlighted in red dashed boxes in Figures 3 and 4. Based on the calculations, we suggest that the third-generation peroxy radical is dominantly the R3OO from the α-abstraction channel, whereas the fourth-generation peroxy radical is the Rβ4OO from the β-abstraction channel. We did not observe signals corresponding to the initial peroxy radicals (R1OO and Rβ1OO) or the peroxy radicals with one hydroperoxy group (R2OO and Rβ2OO), likely due to the predicted very fast H-shift reactions leading rapidly to the higher oxidation products and the expected lower detection sensitivity of these less oxidized/functionalized species.

In both experiments applying either pyruvate or iodide ionization, an unknown compound with a nominal mass of 163 Th (appearing at a nominal mass of 250 Th in Figure 5 and at 290 Th in Figure S8) was detected with a yield of a few percent. This mass is consistent with that of a hydroxy hydroperoxy amide, which could be formed from alkoxy chemistry.

Product Yields in TEA + OH Reaction. In Figure 6, we show the measured (lower limit) product concentration of the dihydroperoxy peroxy radical (R3OO) and dihydroperoxy amide (DHPA) as a function of reacted TEA (Section S4). These signals will also contain small amounts of isomeric compounds arising from the minor β-abstraction channel. Signals from both R3OO and DHPA rise linearly with reacted TEA in agreement with the fast H-shift reactions leading to R3OO. We have assumed negligible bimolecular reaction due to low concentrations of NO and RO_2; the latter due to the small amount of TEA reacted. From the slopes in Figure 6, we obtain a lower limit on the formation yield of 0.29 ± 0.0066 for the R3OO radical and 0.10 ± 0.0024 for DHPA. Stated uncertainties comprise two standard deviations of statistical errors from the regression analysis only. In the corresponding experiment using pyruvate as a reagent ion, we found comparable yields of 0.21 ± 0.0061 and 0.084 ± 0.0018, respectively, for these two products (Figures S9), suggesting high detection sensitivity using both ionization schemes. The overall uncertainties in the lower limit yields are about a factor of 2 based on the expected uncertainties in the calibration factors. Nevertheless, the high combined yield of these two products (expected main products from the calculations) within the 7.9 s reaction window indicates that autoxidation in TEA is indeed fast and dominant similar to what was found for TMA.[12] This is in good agreement with the calculated H-shift rate coefficients in Table 1 and Figures 3 and 4.

By adding more O_3 in the TME ozonolysis experiment to increase the OH concentration and allowing more TEA to react (Figure S9), we determine a small yield of the highly oxidized trihydroperoxy peroxy radical of about 0.0021. Based on our calculations for the major α-abstraction channel, we expect no formation of R4OO via α-abstraction, given the prohibitively slow 1,6 H-shift from the methyl group (Figure 3, k_{3a}). The calculated slow 1,6 H-shift of the methyl hydrogen is consistent with trends observed previously in hydrocarbons.[23] In the β-abstraction channel, the formation of the Rβ4OO radical does not include this slow methyl H-shift but arises from a 1,5 H-shift that is expected to be fast, assuming that the 1,5 H-shift rate coefficients in the β-abstraction channel are comparable to those of the α-abstraction channel. Thus, the observed trihydroperoxy peroxy radical signal likely corresponds to the Rβ4OO radical that originates from the minor β-abstraction channel. Since the Rβ4OO radical signal is very small (Figure S9) and the 1,5 H-shift that forms it is likely fast, the DHPA and Rβ3OO formation from the β-abstraction channel will be small. Thus, we expect that Rβ4OO is the dominant radical formed in the β channel and that the observed dihydroperoxy peroxy radical signal is dominated by the R3OO radical arising from the α-abstraction channel. This is reasonable, as the preceding H-shifts are all expected to be fast. If the sensitivities are comparable, then the yields of R3OO and Rβ4OO should be proportional to the α- and β-abstraction channel yields, respectively. We can then estimate the β-abstraction channel to have a yield of about 0.01. This compares very well with the β-carbon hydrogen abstraction

https://doi.org/10.1021/acs.jpca.3c04341
J. Phys. Chem. A 2023, 127, 8623−8632

yield of about 0.015, estimated from the α- and β-abstraction rate coefficients from an OH hydrogen abstraction SAR.[46]

We modeled the product formation yields at the 7.9 s of the flow-tube experiments for the experiment shown in Figure 6 based on the calculated and estimated rate coefficients for the reactions in Figures 3 and 4 including all stereoisomers (Section S5).[12] The modeling is in agreement with a strong favoring of the initial H-abstraction from the α position. With an α to β ratio of 98:2, the model agrees with the observed very small yields of both HPA and THPA (Figure S10). The model suggests too fast DHPA formation and hence OH recycling. The modeled ratio of R3OO to DHPA is likely too high, suggesting that the calculated k_{3b} values are too high. If we halve k_{3b} values in the modeling, the ratio of R3OO to DHPA becomes close to that observed experimentally (Figure S11). The total modeled yields of R3OO and DHPA are still higher than the lower limit yields of the experiments. Overall, the modeling is in good agreement with experiments and supports the rate coefficients within the uncertainties of both the experiment and calculations.

CONCLUSIONS

We have discovered that autoxidation is a dominating pathway in triethylamine (TEA) + OH oxidation under atmospheric conditions. The multiconformer transition-state theory (MC-TST) calculated the H-shift rate coefficient at 298 K is 25 s^{-1} for the first-generation H-shift in TEA autoxidation. The subsequent peroxy radicals have multiple stereoisomers with a range of H-shift rate coefficients. The second-generation H-shift is 43 s^{-1} for the fastest stereoisomer. The TEA autoxidation leads to the formation of highly oxygenated and functionalized compounds with the O:C ratios larger than one and with as many as three hydroperoxy (OOH) groups. Most of the proposed radicals and closed-shell compounds are detected within the 7.9 s time window of the free-jet flow-tube experiments.

Formation of the most highly oxidized trihydroperoxy compounds is only plausible from the minor channel following OH abstraction at the β-carbon due to a prohibitively slow methyl 1,6 H-shift from the dihydroperoxy peroxy radical in the α-abstraction channel. Combined with measured yields of the dihydroperoxy and trihydroperoxy radicals, we estimate that the β-abstraction channel accounts for at most a few percent.

The autoxidation H-shifts in TEA are even faster than those previously found in trimethylamine (TMA) + OH autoxidation. Thus, autoxidation will likely be the dominant atmospheric oxidation mechanism for most tertiary amines in almost all environments. This will lead to the formation of highly functionalized hydroperoxy amides and likely contribute to secondary organic aerosol (SOA) formation.

ASSOCIATED CONTENT

Supporting Information

The Supporting Information is available free of charge at https://pubs.acs.org/doi/10.1021/acs.jpca.3c04341.

The Supporting Information includes additional theoretical results and details for the MC-TST calculation for both the α- and β-abstraction channels and additional experimental results for different experimental conditions. Output files for all calculations including B3LYP/6-31+G(d) and ωB97X-D/aug-cc-pVTZ xyz-geometries and CCSD(T)-F12a energies are available online at https://erda.ku.dk/archives/c1e147e4db477b9476027926f5a2a1ec/published-archive.html (PDF)

AUTHOR INFORMATION

Corresponding Author

Henrik G. Kjaergaard − *Department of Chemistry, University of Copenhagen, DK-2100 Copenhagen Ø, Denmark;* orcid.org/0000-0002-7275-8297; Email: hgk@chem.ku.dk; Fax: +45-35320322

Authors

Eva R. Kjærgaard − *Department of Chemistry, University of Copenhagen, DK-2100 Copenhagen Ø, Denmark;* Present Address: Department of Chemistry, Aarhus University, Langelandsgade 140, DK-8000 Aarhus C, Denmark; orcid.org/0000-0001-8838-0084

Kristian H. Møller − *Department of Chemistry, University of Copenhagen, DK-2100 Copenhagen Ø, Denmark;* Present Address: Danish Meteorological Institute, Lyngbyvej 100, DK-2100 Copenhagen Ø, Denmark.; orcid.org/0000-0001-8070-8516

Torsten Berndt − *Atmospheric Chemistry Department (ACD), Leibniz Institute for Tropospheric Research (TROPOS), 04318 Leipzig, Germany;* orcid.org/0000-0003-2014-6018

Complete contact information is available at: https://pubs.acs.org/10.1021/acs.jpca.3c04341

Notes

The authors declare no competing financial interest.

ACKNOWLEDGMENTS

The authors thank Jing Chen for the helpful discussions. ERK thanks Ingeniør Alexandre Haynmans og hustru Nina Haynmans Fond, William Demant Fonden, and Københavns Universitets studenterfond for funding her visit to TROPOS to conduct experiments. They thank K. Pielok, R. Gräfe, and A. Rohmer for technical assistance in the experiments and the tofTools team for providing the data analysis tools. The authors are grateful for funding from the Independent Research Fund Denmark (Grant No. 9040-00142B), the Novo Nordisk Foundation Interdisciplinary Synergy Program (Grant No. NNF19OC0057374), and computer time from the High-Performance Center at the Faculty of Science at the University of Copenhagen.

REFERENCES

(1) Peeters, J.; Nguyen, T. L.; Vereecken, L. HOx Radical Regeneration in the Oxidation of Isoprene. *Phys. Chem. Chem. Phys.* **2009**, *11* (28), 5935−5939.

(2) Crounse, J. D.; Nielsen, L. B.; Jørgensen, S.; Kjaergaard, H. G.; Wennberg, P. O. Autoxidation of Organic Compounds in the Atmosphere. *J. Phys. Chem. Lett.* **2013**, *4* (20), 3513−3520.

(3) Vereecken, L.; Müller, J. F.; Peeters, J. Low-Volatility Poly-Oxygenates in the OH-Initiated Atmospheric Oxidation of α-Pinene: Impact of Non-Traditional Peroxyl Radical Chemistry. *Phys. Chem. Chem. Phys.* **2007**, *9* (38), 5241−5248.

(4) Ehn, M.; Thornton, J. A.; Kleist, E.; Sipilä, M.; Junninen, H.; Pullinen, I.; Springer, M.; Rubach, F.; Tillmann, R.; Lee, B.; et al. A Large Source of Low-Volatility Secondary Organic Aerosol. *Nature* **2014**, *506* (7489), 476−479.

(5) Møller, K. H.; Bates, K. H.; Kjaergaard, H. G. The Importance of Peroxy Radical Hydrogen-Shift Reactions in Atmospheric Isoprene Oxidation. *J. Phys. Chem. A* **2019**, *123* (4), 920−932.
(6) Xu, L.; Møller, K. H.; Crounse, J. D.; Otkjær, R. V.; Kjaergaard, H. G.; Wennberg, P. O. Unimolecular Reactions of Peroxy Radicals Formed in the Oxidation of α-Pinene and β-Pinene by Hydroxyl Radicals. *J. Phys. Chem. A* **2019**, *123* (8), 1661−1674.
(7) Wu, R.; Wang, S.; Wang, L. New Mechanism for the Atmospheric Oxidation of Dimethyl Sulfide. The Importance of Intramolecular Hydrogen Shift in a CH_3SCH_2OO Radical. *J. Phys. Chem. A* **2015**, *119* (1), 112−117.
(8) Berndt, T.; Scholz, W.; Mentler, B.; Fischer, L.; Hoffmann, E. H.; Tilgner, A.; Hyttinen, N.; Prisle, N. L.; Hansel, A.; Herrmann, H. Fast Peroxy Radical Isomerization and OH Recycling in the Reaction of OH Radicals with Dimethyl Sulfide. *J. Phys. Chem. Lett.* **2019**, *10* (21), 6478−6483.
(9) Veres, P. R.; Neuman, J. A.; Bertram, T. H.; Assaf, E.; Wolfe, G. M.; Williamson, C. J.; Weinzierl, B.; Tilmes, S.; Thompson, C. R.; Thames, A. B.; et al. Global Airborne Sampling Reveals a Previously Unobserved Dimethyl Sulfide Oxidation Mechanism in the Marine Atmosphere. *Proc. Natl. Acad. Sci. U.S.A.* **2020**, *117* (9), 4505−4510.
(10) Berndt, T.; Chen, J.; Møller, K. H.; Hyttinen, N.; Prisle, N. L.; Tilgner, A.; Hoffmann, E. H.; Herrmann, H.; Kjaergaard, H. G. SO_2 Formation and Peroxy Radical Isomerization in the Atmospheric Reaction of OH Radicals with Dimethyl Disulfide. *Chem. Commun.* **2020**, *56* (88), 13634−13637.
(11) Møller, K. H.; Berndt, T.; Kjaergaard, H. G. Atmospheric Autoxidation of Amines. *Environ. Sci. Technol.* **2020**, *54* (18), 11087−11099.
(12) Berndt, T.; Møller, K. H.; Herrmann, H.; Kjaergaard, H. G. Trimethylamine Outruns Terpenes and Aromatics in Atmospheric Autoxidation. *J. Phys. Chem. A* **2021**, *125* (20), 4454−4466.
(13) Ye, Q.; Goss, M. B.; Isaacman-VanWertz, G.; Zaytsev, A.; Massoli, P.; Lim, C.; Croteau, P.; Canagaratna, M.; Knopf, D. A.; Keutsch, F. N.; et al. Organic Sulfur Products and Peroxy Radical Isomerization in the OH Oxidation of Dimethyl Sulfide. *ACS Earth Space Chem.* **2021**, *5* (8), 2013−2020.
(14) Almeida, J.; Schobesberger, S.; Kürten, A.; Ortega, I. K.; Kupiainen-Määttä, O.; Praplan, A. P.; Adamov, A.; Amorim, A.; Bianchi, F.; Breitenlechner, M.; et al. Molecular Understanding of Sulphuric Acid−Amine Particle Nucleation in the Atmosphere. *Nature* **2013**, *502* (7471), 359−363.
(15) Bianchi, F.; Kurtén, T.; Riva, M.; Mohr, C.; Rissanen, M. P.; Roldin, P.; Berndt, T.; Crounse, J. D.; Wennberg, P. O.; Mentel, T. F.; et al. Highly Oxygenated Organic Molecules (HOM) from Gas-Phase Autoxidation Involving Peroxy Radicals: A Key Contributor to Atmospheric Aerosol. *Chem. Rev.* **2019**, *119* (6), 3472−3509.
(16) Andreae, M. O. Ocean-Atmosphere Interactions in the Global Biogeochemical Sulfur Cycle. *Mar. Chem.* **1990**, *30*, 1−29.
(17) Novak, G. A.; Kilgour, D. B.; Jernigan, C. M.; Vermeuel, M. P.; Bertram, T. H. Oceanic Emissions of Dimethyl Sulfide and Methanethiol and their Contribution to Sulfur Dioxide Production in the Marine Atmosphere. *Atmos. Chem. Phys.* **2022**, *22* (9), 6309−6325.
(18) Ge, X.; Wexler, A. S.; Clegg, S. L. Atmospheric amines − Part I. A Review. *Atmos. Environ.* **2011**, *45* (3), 524−546.
(19) Ma, F.; Xie, H.-B.; Li, M.; Wang, S.; Zhang, R.; Chen, J. Autoxidation Mechanism for Atmospheric Oxidation of Tertiary Amines: Implications for Secondary Organic Aerosol Formation. *Chemosphere* **2021**, *273*, No. 129207.
(20) Nielsen, C. J.; Herrmann, H.; Weller, C. Atmospheric Chemistry and Environmental Impact of the use of Amines in Carbon Capture and Storage (CCS). *Chem. Soc. Rev.* **2012**, *41* (19), 6684−6704.
(21) Jenkin, M. E.; Valorso, R.; Aumont, B.; Rickard, A. R. Estimation of Rate Coefficients and Branching Ratios for Reactions of Organic Peroxy Radicals for Use in Automated Mechanism Construction. *Atmos. Chem. Phys.* **2019**, *19* (11), 7691−7717.
(22) Chen, J.; Møller, K. H.; Wennberg, P. O.; Kjaergaard, H. G. Unimolecular Reactions Following Indoor and Outdoor Limonene Ozonolysis. *J. Phys. Chem. A* **2021**, *125* (2), 669−680.
(23) Otkjær, R. V.; Jakobsen, H. H.; Tram, C. M.; Kjaergaard, H. G. Calculated Hydrogen Shift Rate Constants in Substituted Alkyl Peroxy Radicals. *J. Phys. Chem. A* **2018**, *122* (43), 8665−8673.
(24) Berndt, T.; Chen, J.; Kjærgaard, E. R.; Møller, K. H.; Tilgner, A.; Hoffmann, E. H.; Herrmann, H.; Crounse, J. D.; Wennberg, P. O.; Kjaergaard, H. G. Hydrotrioxide (ROOOH) Formation in the Atmosphere. *Science* **2022**, *376* (6596), 979−982.
(25) Vereecken, L.; Peeters, J. The 1,5-H-Shift in 1-Butoxy: A Case Study in the Rigorous Implementation of Transition State Theory for a Multirotamer System. *J. Chem. Phys.* **2003**, *119* (10), 5159−5170.
(26) Møller, K. H.; Otkjær, R. V.; Hyttinen, N.; Kurtén, T.; Kjaergaard, H. G. Cost-Effective Implementation of Multiconformer Transition State Theory for Peroxy Radical Hydrogen Shift Reactions. *J. Phys. Chem. A* **2016**, *120* (51), 10072−10087.
(27) Praske, E.; Otkjær, R. V.; Crounse, J. D.; Hethcox, J. C.; Stoltz, B. M.; Kjaergaard, H. G.; Wennberg, P. O. Atmospheric Autoxidation is Increasingly Important in Urban and Suburban North America. *Proc. Natl. Acad. Sci. U.S.A.* **2018**, *115* (1), 64−69.
(28) Lee, C.; Yang, W.; Parr, R. G. Development of the Colle-Salvetti Correlation-Energy Formula into a Functional of the Electron Density. *Phys. Rev. B* **1988**, *37* (2), 785.
(29) Clark, T.; Chandrasekhar, J.; Spitznagel, G. W.; Schleyer, P. V. R. Efficient Diffuse Function-Augmented Basis Sets for Anion Calculations. III. The 3-21+G Basis Set for First-Row Elements, Li−F. *J. Comput. Chem.* **1983**, *4* (3), 294−301.
(30) Becke, A. D. Density-Functional Thermochemistry. III. The Role of Exact Exchange. *J. Chem. Phys.* **1993**, *98*, 5646−5648.
(31) Frisch, M. J.; Trucks, G. W.; Schlegel, H. B.; Scuseria, G. E.; Robb, M. A.; Cheeseman, J. R.; Scalmani, G.; Barone, V.; Petersson, G. A.; Nakatsuji, H.. et al.*Gaussian 16 Rev. B.01*; Wallingford, CT, 2016.
(32) *Spartan'14*; Wavefunction Inc.; Irvine, 2014.
(33) Halgren, T. A. Merck Molecular Force Field. I. Basis, Form, Scope, Parameterization, and Performance of MMFF94. *J. Comput. Chem.* **1996**, *17* (5−6), 490−519.
(34) Otkjær, R.; Møller, K. H. Removal of Duplicate Conformers, 2018, https://github.com/TheKjaergaardGroup/Removal-of-Duplicate-Conformers.
(35) Chai, J.-D.; Head-Gordon, M. Long-Range Corrected Hybrid Density Functionals with Damped Atom−Atom Dispersion Corrections. *Phys. Chem. Chem. Phys.* **2008**, *10* (44), 6615−6620.
(36) Dunning, T. H., Jr Gaussian Basis Sets for Use in Correlated Molecular Calculations. I. The Atoms Boron Through Neon and Hydrogen. *J. Chem. Phys.* **1989**, *90* (2), 1007−1023.
(37) Adler, T. B.; Knizia, G.; Werner, H.-J. A Simple and Efficient CCSD(T)-F12 Approximation. *J. Chem. Phys.* **2007**, *127* (22), No. 221106.
(38) Werner, H.; Knowles, P.; Knizia, G.; Manby, F.; Schütz, M.; Celani, P.; Korona, T.; Lindh, R.; Mitrushenkov, A.; Rauhut, G. *MOLPRO, version 2012.1, a Package of Ab Initio Programs, 2012*; 2012.
(39) Eckart, C. The Penetration of a Potential Barrier by Electrons. *Phys. Rev.* **1930**, *35* (11), 1303−1309.
(40) Møller, K. H.; Praske, E.; Xu, L.; Crounse, J. D.; Wennberg, P. O.; Kjaergaard, H. G. Stereoselectivity in Atmospheric Autoxidation. *J. Phys. Chem. Lett.* **2019**, *10* (20), 6260−6266.
(41) Kroll, J. H.; Sahay, S. R.; Anderson, J. G.; Demerjian, K. L.; Donahue, N. M. Mechanism of HOx Formation in the Gas-Phase Ozone-Alkene Reaction. 2. Prompt versus Thermal Dissociation of Carbonyl Oxides to Form OH. *J. Phys. Chem. A* **2001**, *105* (18), 4446−4457.
(42) Raff, J. D.; Finlayson-Pitts, B. J. Hydroxyl Radical Quantum Yields from Isopropyl Nitrite Photolysis in Air. *Environ. Sci. Technol.* **2010**, *44* (21), 8150−8155.
(43) Berndt, T.; Richters, S.; Jokinen, T.; Hyttinen, N.; Kurtén, T.; Otkjær, R. V.; Kjaergaard, H. G.; Stratmann, F.; Herrmann, H.; Sipilä,

https://doi.org/10.1021/acs.jpca.3c04341
J. Phys. Chem. A 2023, 127, 8623−8632

M.; et al. Hydroxyl Radical-Induced Formation of Highly Oxidized Organic Compounds. *Nat. Commun.* **2016**, *7* (1), No. 13677.
(44) Berndt, T.; Hyttinen, N.; Herrmann, H.; Hansel, A. First Oxidation Products from the Reaction of Hydroxyl Radicals with Isoprene for Pristine Environmental Conditions. *Commun. Chem.* **2019**, *2*, 21.
(45) Onel, L.; Thonger, L.; Blitz, M. A.; Seakins, P. W.; Bunkan, A. J. C.; Solimannejad, M.; Nielsen, C. J. Gas-Phase Reactions of OH with Methyl Amines in the Presence or Absence of Molecular Oxygen. An Experimental and Theoretical Study. *J. Phys. Chem. A* **2013**, *117* (41), 10736−10745.
(46) Kwok, E. S. C.; Atkinson, R. Estimation of Hydroxyl Radical Reaction Rate Constants for Gas-Phase Organic Compounds Using a Structure-Reactivity Relationship: An Update. *Atmos. Environ.* **1995**, *29* (14), 1685−1695.
(47) Park, J.; Jongsma, C. G.; Zhang, R.; North, S. W. OH/OD Initiated Oxidation of Isoprene in the Presence of O_2 and NO. *J. Phys. Chem. A* **2004**, *108* (48), 10688−10697.
(48) Kjærgaard, E. R.; Holten, K. H.; Kjaergaard, H. G. Atmospheric Oxidation of Hydroxyperoxy Amides. *J. Phys. Chem. A*, in press.
(49) Allen, H. M.; Crounse, J. D.; Bates, K. H.; Teng, A. P.; Krawiec-Thayer, M. P.; Rivera-Rios, J. C.; Keutsch, F. N.; St Clair, J. M.; Hanisco, T. F.; Møller, K. H.; et al. Kinetics and Product Yields of the OH Initiated Oxidation of Hydroxymethyl Hydroperoxide. *J. Phys. Chem. A* **2018**, *122* (30), 6292−6302.
(50) Glowacki, D. R.; Liang, C.-H.; Morley, C.; Pilling, M. J.; Robertson, S. H. MESMER: An Open-Source Master Equation Solver for Multi-Energy Well Reactions. *J. Phys. Chem. A* **2012**, *116* (38), 9545−9560.
(51) Jørgensen, S.; Knap, H. C.; Otkjær, R. V.; Jensen, A. M.; Kjeldsen, M. L. H.; Wennberg, P. O.; Kjaergaard, H. G. Rapid Hydrogen Shift Scrambling in Hydroperoxy-Substituted Organic Peroxy Radicals. *J. Phys. Chem. A* **2016**, *120* (2), 266−275.
(52) Murphy, S. M.; Sorooshian, A.; Kroll, J. H.; Ng, N. L.; Chhabra, P.; Tong, C.; Surratt, J. D.; Knipping, E.; Flagan, R. C.; Seinfeld, J. H. Secondary Aerosol Formation from Atmospheric Reactions of Aliphatic Amines. *Atmos. Chem. Phys.* **2007**, *7* (9), 2313−2337.
(53) Price, D. J.; Clark, C. H.; Tang, X.; Cocker, D. R.; Purvis-Roberts, K. L.; Silva, P. J. Proposed Chemical Mechanisms Leading to Secondary Organic Aerosol in the Reactions of Aliphatic Amines with Hydroxyl and Nitrate Radicals. *Atmos. Environ.* **2014**, *96*, 135−144.
(54) Price, D. J.; Kacarab, M.; Cocker, D. R.; Purvis-Roberts, K. L.; Silva, P. J. Effects of Temperature on the Formation of Secondary Organic Aerosol from Amine Precursors. *Aerosol Sci. Technol.* **2016**, *50* (11), 1216−1226.

https://doi.org/10.1021/acs.jpca.3c04341
J. Phys. Chem. A 2023, 127, 8623−8632